



## Original articles

Research article

<https://doi.org/10.17308/kcmf.2022.24/9861>

## Influence of the method of formation a nanosized $\text{CoFe}_2\text{O}_4$ /nontronite composite on its structure and properties

E. V. Tomina<sup>1,2✉</sup>, N. A. Khodosova<sup>2</sup>, A. A. Sinelnikov<sup>1</sup>, A. V. Zhabin<sup>1</sup>, N. A. Kurkin<sup>1</sup>, L. A. Novikova<sup>2</sup>

<sup>1</sup>Voronezh State University,  
1 Universitetskaya pl., Voronezh 394018, Russian Federation

<sup>2</sup>Voronezh State University of Forestry and Technologies named after G. F. Morozov  
8 Timiryazeva str., Voronezh 394087, Russian Federation

### Abstract

The aim of the study was to establish the influence of the method of formation of the  $\text{CoFe}_2\text{O}_4$ /nontronite nanocomposite on its structure and properties.

Impurity-free nanoparticles of cobalt ferrite  $\text{CoFe}_2\text{O}_4$  (XRD), close to spherical in shape, with a predominant particle fraction in the range of 8–20 nm (TEM), were synthesized using the citrate combustion method. The formation of the  $\text{CoFe}_2\text{O}_4$ /nontronite nanocomposite was carried out by two methods: mechanical mixing of available precursors followed by annealing and combustion of iron-cobalt citrate with the formation of spinel in the presence of nontronite in the reactor.

The  $\text{CoFe}_2\text{O}_4$ /nontronite nanocomposite formed by the first method is characterized by the decomposition of natural aluminosilicate aggregates and a higher sorption activity with respect to formaldehyde than the original clay mineral and spinel. The second method of composite formation leads to the formation of coarse-grained silica structures with worse sorption activity in comparison with natural aluminosilicate and  $\text{CoFe}_2\text{O}_4$ .

**Keywords:** Nanocomposite, Citrate combustion method, Cobalt ferrite, Aluminosilicate

**Funding:** the research results were partially obtained using the equipment of the Centre for Collective Use of Scientific Equipment of Voronezh State University. URL: <http://ckp.vsu.ru>.

**For citation:** Tomina E. V., Khodosova N. A., Sinelnikov A. A., Zhabin A. V., Kurkin N. A., Novikova L. A. Influence of the method of formation a nanosized  $\text{CoFe}_2\text{O}_4$ /nontronite composite on its structure and properties *Condensed Matter and Interphases*. 2022;24(3): 379–386. <https://doi.org/10.17308/kcmf.2022.24/9861>

**Для цитирования:** Томина Е. В., Ходосова Н. А., Синельников А. А., Жабин А. В., Куркин Н. А., Новикова Л. А. Влияние метода формирования композита наноразмерный  $\text{CoFe}_2\text{O}_4$ /нонтронит на его структуру и свойства. *Конденсированные среды и межфазные границы*. 2022;24(3): 379–386. <https://doi.org/10.17308/kcmf.2022.24/9861>

✉ Elena V. Tomina, e-mail: [tomina-ev@yandex.ru](mailto:tomina-ev@yandex.ru)

© Tomina E. V., Khodosova N. A., Sinelnikov A. A., Zhabin A. V., Kurkin N. A., Novikova L. A., 2022



The content is available under Creative Commons Attribution 4.0 License.

## 1. Introduction

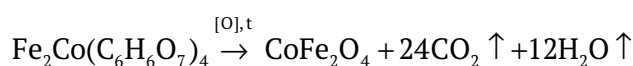
Demand for nanosized ferrites as magnetic materials [1, 2], catalysts [3], and recently also as sorbents [4], is determined, first of all, by the possibility of controlling their magnetic, structural, catalytic, and sorption characteristics by changing the methods for synthesizing nanocrystals and doping them with various cations [5–9]. Catalysts based on nanosized ferrites are significantly cheaper than those based on platinum and rare earth metals, precursors for their manufacture are readily available, and synthesis methods are reproducible and scalable [1, 2]. The prospects of using  $\text{MeFe}_2\text{O}_4$  (Me = Co, Ni, Zn, Cu) as catalysts and sorbents is also determined by their chemical stability in acidic environments, thermal and temporal stability, highly developed surface, high saturation magnetization and residual magnetization, which opens up the possibility of their extraction by magnetic separation methods [10, 11]. In the areas of catalysis and sorption, composite materials based on a less expensive dispersed matrix and nanosized ferrite as a magnetic component are often used. The clay mineral nontronite, which is a highly dispersed natural sorbent, was chosen as the basis for the composite. The structure of nontronite is represented by a three-layer package, including two layers of silicon-oxygen tetrahedra separated by one octahedral  $\text{FeO}_6$  package, between which water molecules with exchangeable cations are located [12]. The chemical composition of nontronite is variable, the most probable formula is  $\text{Fe}_2^{3+}[\text{Al}_x\text{Si}_{4-x}\text{O}_{10}](\text{OH})_2 \cdot \text{Na}_{0.33}(\text{H}_2\text{O})$  [13]. The mineral from the Voronezh deposit (Russia), which, according to [14], contains 80% of nontronite and 10% of illite and kaolinite was used in the study.

The aim of the study was to establish the influence of the method of formation of the  $\text{CoFe}_2\text{O}_4$ /nontronite nanocomposite on its structure and properties.

## 2. Experimental

The synthesis of ferrite-spinel  $\text{CoFe}_2\text{O}_4$  using the citrate combustion method was carried out according to [15]. The first approach to the formation of the  $\text{CoFe}_2\text{O}_4$ /nontronite nanocomposite consisted of mechanical mixing the available precursors followed by annealing

(method 1). To obtain a composite material, 20 wt. % cobalt ferrite and 80 wt. % nontronite, a small amount of ethanol was added to the mixture and mixed thoroughly. The resulting paste was air dried for 2 h and annealed in a muffle furnace (SNOL 8.2/1100) to remove alcohol at 500°C for 1 h. The second method for the formation of a composite (method 2) consisted in preparing a solution of iron citrate and cobalt citrate according to [15]. Then nontronite with the weight required to form a composite with the composition 20%  $\text{CoFe}_2\text{O}_4$ /80% nontronite was added to the solution. The reaction mixture was heated until the water had completely evaporated. In this case, a grey-red paste, a mixture of nontronite and iron-cobalt citrate was formed. During further heating, the decomposition of iron-cobalt citrate occurred with the formation of cobalt ferrite:



The resulting dark grey insoluble powder was annealed in a muffle furnace (SNOL 8.2/1100) to remove water at 300°C for 1 h.

Phase composition of the cobalt ferrite and the  $\text{CoFe}_2\text{O}_4$ /nontronite composite were studied by X-ray diffractometry (XRD, Empyrean BV diffractometer with Cu anode ( $\lambda = 1.54060$  nm)). The scanning was performed within a range of angles  $2\theta = 10\text{--}80^\circ$  with a step of 0.0200. The JCPDC database [16] was used to identify the phases. The size of the coherent scattering regions of the  $\text{CoFe}_2\text{O}_4$  particles based on the broadening of X-ray diffraction lines calculated using the Debye-Scherrer formula (1) [17]:

$$D_{\text{hkl}} = \frac{kx\lambda}{\beta_{\text{hkl}} \times \cos\theta}, \quad (1)$$

where  $D_{\text{hkl}}$  is the average particle size, Å,  $k$  is the correction factor (for spherical particles  $k = 0.9$ ),  $\lambda$  is the X-ray tube wavelength,  $\theta$  is the position of the peak maximum, deg.,  $\beta_{\text{hkl}}$  is the intrinsic physical broadening of the diffraction maximum, rad.

The size and morphology of the composite particles synthesized by different methods was determined based on the data of transmission electron microscopy (TEM, transmission electron microscope CarlZeiss Libra-120). The particle size distribution histogram was plotted using the ImageJ program version 1.53k.

The sorption capacity of natural nontronite, pure  $\text{CoFe}_2\text{O}_4$  and  $\text{CoFe}_2\text{O}_4$ /nontronite nanocomposite was tested in relation to formaldehyde, a toxicant of the 2nd hazard class [18]. For the determination of the sorption capacity  $0.025 \text{ dm}^3$  formaldehyde solution were added to 0.5 g of the composite, the static sorption time was 2 h. After the end of sorption, the solution was filtered. The content of formaldehyde in the filtrate was determined using the sulphite method. The relative error of determination was 1–3%.

### 3. Results and discussion

According to XRD data (Fig. 1), the cobalt ferrite sample synthesized by the citrate method is completely single-phase. All reflections in the diffraction pattern corresponded to that of cobalt ferrite with a  $\text{CoFe}_2\text{O}_4$  spinel structure [16].

According to TEM data (Fig. 2), the cobalt ferrite particles had a shape close to spherical, and agglomeration was clearly expressed. The particle size was in the range from 6 to 34 nm. The predominant particle size fraction was in the range of 8–24 nm.

Nontronite belongs to layered silicates of the group of clay-like smectite minerals [19]. Nontronite is usually found in the form of finely dispersed scaly, vermiform, radial-spherical mineral aggregates, which was confirmed by the TEM data (Fig. 3).

Nontronite aggregates were characterized by layered formations up to 100 nm wide, elongated

in one direction (Fig. 3a). The dark-field image confirmed the ultrafine nature of nontronite mineral aggregates. At the same time, rounded particles with a size of about 10–20 nm could be seen in the images, which was probably a consequence of the insignificant decomposition of nontronite microaggregates into individual flakes as the result of the dispersion during sample preparation.

The  $\text{CoFe}_2\text{O}_4$ /nontronite nanocomposite, synthesized as a mechanical mixture of available precursors, was presented by separate round-shaped particles up to 20 nm in size, probably predominantly crystalline. As can be seen from the TEM image, there were no clay particles of the natural layered shape characteristic of nontronite, which probably was associated with the decomposition of natural aluminosilicate aggregates into individual flakes during nanocomposite annealing. Insignificant agglomeration of particles was expressed. The particle size of the composite did not exceed 20 nm. The predominant particle size fraction was in the size range of 6–12 nm.

The general scheme of dehydration of smectites during heating according to [20] is as follows: interlayer water is almost completely released at 250–300 °C, then a slow release of constitutional water (OH-groups) starts, which ends completely at  $T \sim 750$  °C. The process of dehydration is partially reversible, until it is fully completed. Complete destruction of the structure usually

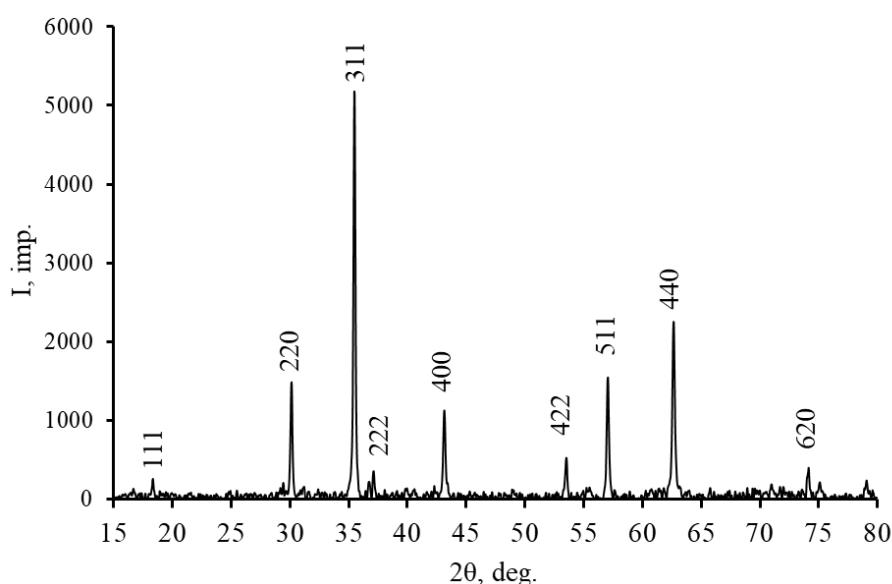
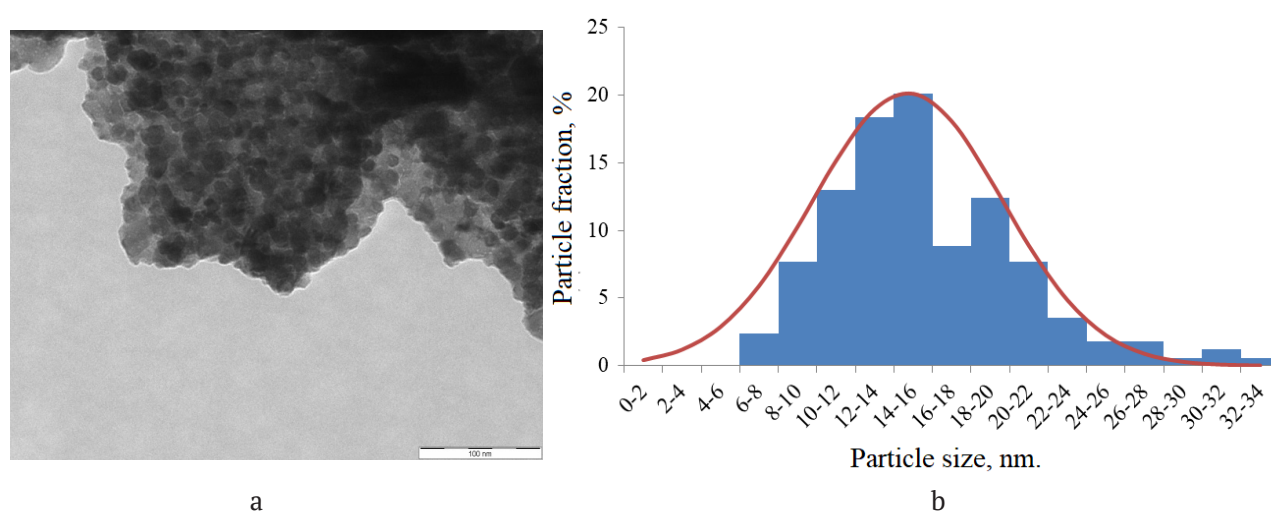
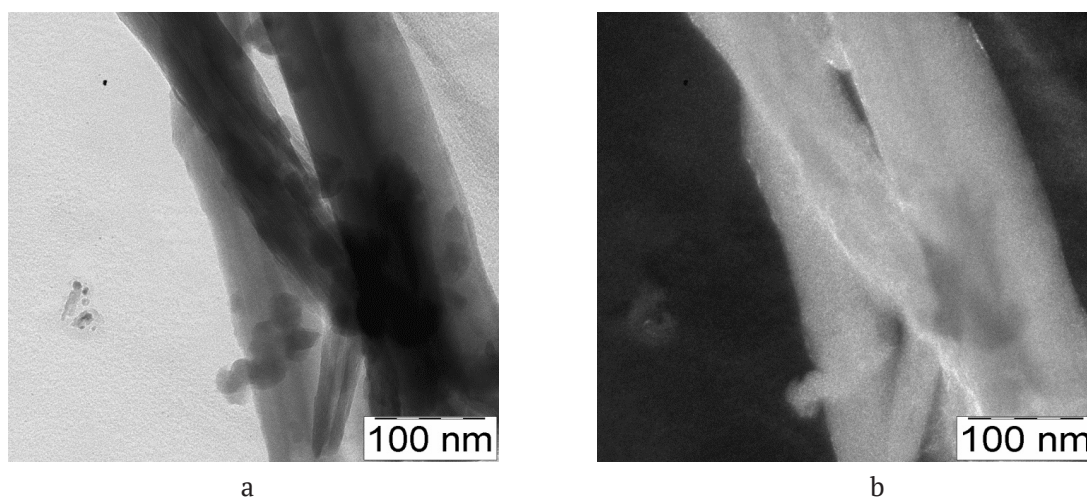


Fig. 1. X-ray diffraction pattern of a  $\text{CoFe}_2\text{O}_4$  sample synthesized by the citrate method



**Fig. 2.** TEM image (a) and particle size distribution histogram (b) of  $\text{CoFe}_2\text{O}_4$



**Fig. 3.** TEM image of nontronite (a) and dark-field image (b)

occurs in the range of 800–900°C. Later studies [21] showed that the process of smectite dehydration is more complex. The transition boundaries are vaguer and do not have clear and stable values on the temperature scale, the transition stages are determined by temperature intervals. For nontronite, dehydroxylation starts already in the range of 400–500°C. At the same time the layered structure is preserved, however, the interlayer spaces are destroyed, the surface area and porosity are reduced. The layered silicate completely loses water and contracts with the formation of micaceous structure with heat treatment at 550 °C. X-ray diffraction patterns of dehydroxylates were quite blurred, XRD study demonstrated the gradual degradation of minerals.

On the diffraction pattern of the  $\text{CoFe}_2\text{O}_4$ /nontronite nanocomposite formed by method 1 (Fig. 5, diffraction pattern 3), all the main

reflections of the cobalt spinel were identified (Fig. 5, diffraction pattern 2). Despite the fact that the conditions for recording the diffraction patterns of the composite did not allow to identify one of the main reflections of nontronite in the region of 5°, the remaining reflections can be identified according to the JCPDC database (Fig. 5, diffraction pattern 1), but their relative intensity was significantly reduced. This finding indicates a general increase in the defectiveness of the structure and dispersion of particles and may be associated with the destruction of aggregates of natural aluminosilicate, the loss of water due to the dehydration processes and partial dehydroxylation.

A completely different diffraction pattern was characteristic of the nanocomposite formed by method 2 (Fig. 5, diffraction pattern 4). The absence of cobalt ferrite reflections indicated that the spinel formed during the combustion of

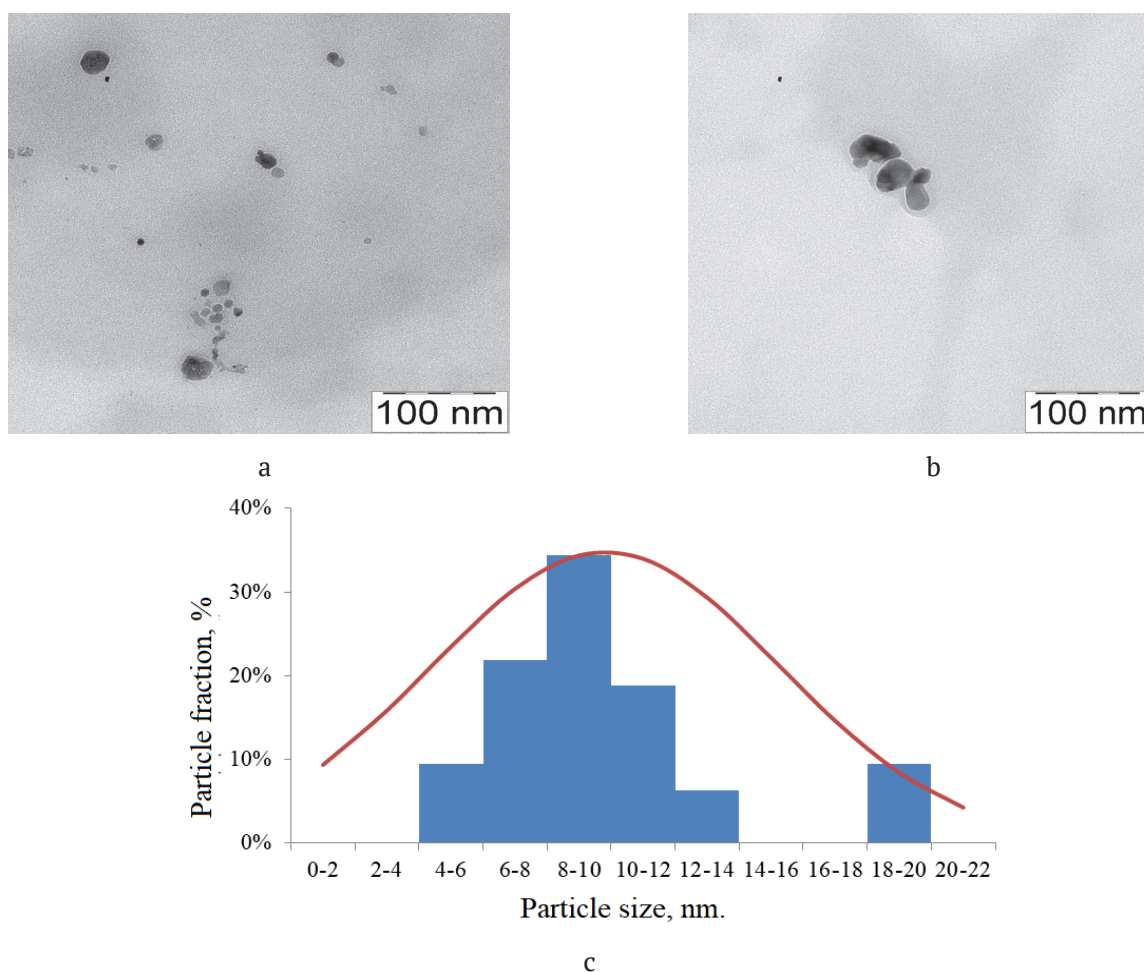


**Fig 4.** TEM image of a  $\text{CoFe}_2\text{O}_4$ /nontronite nanocomposite synthesized by method 1, (a), (b) and particle size distribution histogram (c)

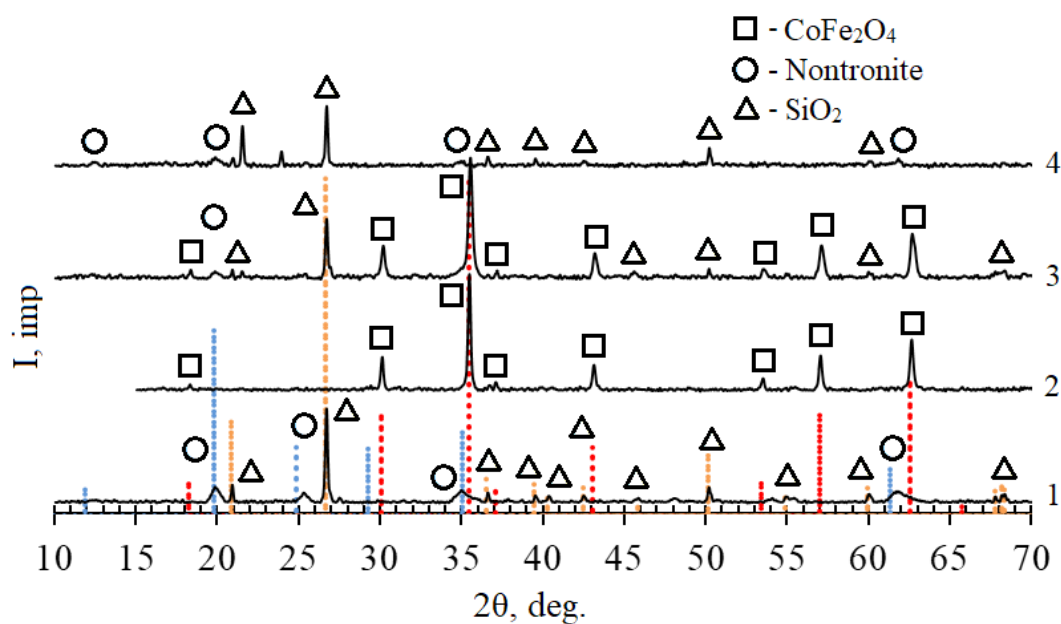


**Fig. 5.** X-ray diffraction pattern of samples of nontronite (1), spinel  $\text{CoFe}_2\text{O}_4$  (2), nanocomposite  $\text{CoFe}_2\text{O}_4$ /nontronite, method 1 (3), nanocomposite  $\text{CoFe}_2\text{O}_4$ /nontronite, method 2 (4)

the polymer gel was predominantly in the X-ray amorphous state. At the same time, reflections of  $\text{SiO}_2$  in the form of quartz, which were also present in the diffraction pattern of natural nontronite, were identified. However, in the region of the diffraction angle of  $22^\circ$ , according to ICDD PDF, the most intense reflection of cristobalite was identified. This reflection was absent in the diffraction patterns of both the natural aluminosilicate and  $\text{CoFe}_2\text{O}_4$ /nontronite composite synthesized by method 1. Probably, the transition of quartz to cristobalite occurs during the combustion of gel-like iron-cobalt citrate under strongly non equilibrium conditions. The possibility of forming a metastable cristobalite at relatively low temperatures outside the classical equilibrium transition scheme quartz - tridymite - cristobalite was also emphasized in [22]. During further heating, metacristobalite transformed into tridymite and then into stable cristobalite.

On the TEM image (Fig. 6) of the  $\text{CoFe}_2\text{O}_4$ /nontronite nanocomposite synthesized by method 2, the overlapping of fairly large flat-crystalline objects up to 400 nm in size can be seen. This was a consequence of the dehydroxylation of nontronite and the formation of a micaceous structure. High iron content, according to [23], is the reason for the relatively low thermal stability of nontronite. A peculiar net structure from chequered holes can be seen at the bottom of Fig. 6b. Such formation is characteristic of the skeletal remains of some species of diatoms. On the

image for Fig. 6a, which was reordered at a lower magnification, parallel dark stripes are visible in its upper right corner. These strips represent a fragment of the skeleton of another diatom species. Colloidal solutions (sols) of silica serve as food for diatoms and it contributes to the perfect preservation of skeletons of these organisms in a fossil state even in the most ancient deposits.

Pure nontronite, cobalt spinel  $\text{CoFe}_2\text{O}_4$  and composites formed by methods 1 and 2 were tested as formaldehyde sorbents (Table 1). Cobalt ferrite had the weakest sorption activity towards formaldehyde, determined based on the value of specific adsorption ( $a = 13 \text{ mg/g}$ ). For natural nontronite, the adsorption capacity is higher -  $27 \text{ mg/g}$ . Formaldehyde adsorption on  $\text{CoFe}_2\text{O}_4$ /nontronite composite synthesized by method 1 exceeded that on cobalt ferrite and pure nontronite ( $a = 30 \text{ mg/g}$ ). For the  $\text{CoFe}_2\text{O}_4$ /nontronite formed by method 2, the value of specific sorption at all formaldehyde concentrations was lower than that of nontronite and composite synthesized by method 1. This was caused, first of all, by the dehydroxylation of nontronite during the synthesis of the composite, which led to the destruction of the octahedral layer and a strong decrease in porosity.

Thus, the first method of forming a composite based on nontronite with the addition of cobalt ferrite opens up prospects for obtaining economically efficient sorbents sensitive to an external magnetic field.

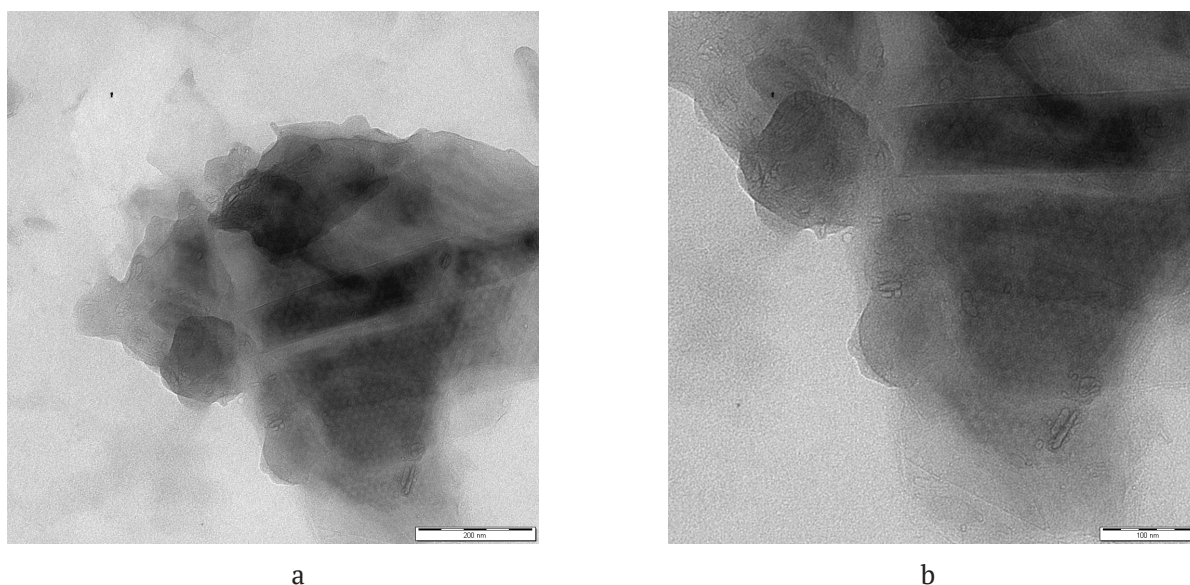


**Fig. 6.** TEM image of the  $\text{CoFe}_2\text{O}_4$ /nontronite nanocomposite synthesized by method 2

**Table 1.** Sorption capacity of nontronite, cobalt ferrite, and composites based on them with respect to formaldehyde solutions of various concentrations

Sample	Specific adsorption, mg/g			
	0.038 M	0.102 M	0.201 M	0.388 M
Nontronite	3.15	14.2	20.8	27.0
CoFe <sub>2</sub> O <sub>4</sub>	4.2	10.5	11.2	13.2
CoFe <sub>2</sub> O <sub>4</sub> /Nontronite method 1	4.1	15.6	22.6	30
CoFe <sub>2</sub> O <sub>4</sub> /Nontronite method 2	4.0	12.0	19.5	22.5

#### 4. Conclusions

The impurity-free cobalt ferrite nanopowder with a predominant particle fraction in the range of 8–24 nm was synthesized using the citrate combustion method. Two methods for the formation of 20 % CoFe<sub>2</sub>O<sub>4</sub>/80 % nontronite nanocomposite were proposed for the production of inexpensive magnetically active sorbent. The effect of synthesis methods on the composition, structure of the composite, and sorption activity with respect to formaldehyde solutions of various concentrations has been established. The CoFe<sub>2</sub>O<sub>4</sub>/nontronite nanocomposite formed by mechanical mixing of available precursors followed by annealing, despite the destruction of submicroaggregates of natural nontronite and partial dehydroxylation, is a more effective sorbent compared to the original clay mineral. The formation of a composite by combustion of iron-cobalt citrate in the presence of nontronite led to the formation of coarse-grained silica structures with worse sorption activity compared to natural aluminosilicate.

#### Author contributions

All authors made an equivalent contribution to the preparation of the publication.

#### Conflict of interests

The authors declare that they have no known competing financial interests or personal relationships that could have influenced the work reported in this paper.

#### References

1. Kefeni K. K., Msagati A. M., Mamba B. B. Ferrite nanoparticles: synthesis, characterisation and applications in electronic device. *Materials Science and Engineering B*. 2017;215: 37–55. <http://dx.doi.org/10.1016/j.mseb.2016.11.002>
2. Tomina E. V., Mittova I. Y., Stekleneva O. V., Kurkin N. A., Perov N. S., Alekhina Y. A. Microwave

synthesis and magnetic properties of bismuth ferrite nanopowder doped with cobalt. *Russian Chemical Bulletin*. 2020;69(5): 941–946. <https://doi.org/10.1007/s11172-020-2852-1>

3. Leila Roshanfekar Rad, Babak Farshi Ghazani, Mohammad Irani, Mohammad Sadegh Sayyafan, Ismaeil Haririan. Comparison study of phenol degradation using cobalt ferrite nanoparticles synthesized by hydrothermal and microwave methods. *Desalination and Water Treatment*. 2014;56(12): 1–10. <https://doi.org/10.1080/19443994.2014.977960>

4. Tkachenko I. A., Panasenko A. E., Odinokov M. M., Marchenko Y. V. Magnetoactive composite sorbents CoFe<sub>2</sub>O<sub>4</sub>-SiO<sub>2</sub>. *Russian Journal of Inorganic Chemistry*. 2020;65(8): 1142–1149. <https://doi.org/10.1134/S0036023620080173>

5. Mittova I. Ya., Perov N. S., Tomina E. V., Pan'kov V. V., Sladkoyevtsev B. V. Multiferroic nanocrystals and diluted magnetic semiconductors as a base for designing magnetic materials. *Inorganic Materials*. 2021;57(13): 22–48. <https://doi.org/10.1134/S0020168521130033>

6. Rashidi S., Ataie A. One-step synthesis of CoFe<sub>2</sub>O<sub>4</sub> nano-particles by mechanical alloying. *Advanced Materials Research*. 2014;829: P. 747–751. <https://doi.org/10.4028/www.scientific.net/AMR.829.747>

7. Agú U. A., Oliva M. I., Marchetti S. G., Heredia A. C., Casuscelli S. G., Crivello M. E. Synthesis and characterization of a mixture of CoFe<sub>2</sub>O<sub>4</sub> and MgFe<sub>2</sub>O<sub>4</sub> from layered double hydroxides: band gap energy and magnetic responses. *Journal of Magnetism and Magnetic Materials*. 2014;369: 249–259. <https://doi.org/10.1016/j.jmmm.2014.06.046>

8. Rao K. S., Nayakulu S. V. R., Varma M. C., Choudary G. S. V. R. K., Rao K. H. Controlled phase evolution and the occurrence of single domain CoFe<sub>2</sub>O<sub>4</sub> nanoparticles synthesized by PVA assisted sol-gel method. *Journal of Magnetism and Magnetic Materials*. 2018;451(1): 602–608. <https://doi.org/10.1016/j.jmmm.2017.11.069>

9. Tomina E. V., Pavlenko A. A., Kurkin N. A. Synthesis of bismuth ferrite nanopowder doped with erbium ions. *Condensed Matter and Interphases*. 2021;23(1): 93–100. <https://doi.org/10.17308/kcmf.2021.23/3309>

10. Rehman F., Sayed M., Khan J. A., Shah L. A., Shah N. S., Khan H. M., Khattak R. Degradation of crystal violet dye by fenton and photo-fenton oxidation processes. *Zeitschrift Fur Physikalische Chemie*. 2018;232(12): 1771–1786. <https://doi.org/10.1515/zpch-2017-1099>
11. Indu Sharma Somnath, Kotnala R. K., Singh M., Kumar Arun, Dhiman Pooja, Singh Virender Pratap, Verma Kartikey, Kumar Gagan. Structural magnetic and mössbauer studies of Nd-doped Mg-Mn ferrite nanoparticles. *Journal of Magnetism and Magnetic Materials*. 2017;444: 77–86. <https://doi.org/10.1016/j.jmmm.2017.08.017>
12. Tsipursky S. I., Drits V. A., Chekin S. S. Revealing the structural ordering of nontronites by the oblique texture electron diffraction method. *Proceedings of the Academy of Sciences of the USSR, geological series*. 1978;10: 105–113. (In Russ.)
13. Al-Ahmed A. (Ed.). Advanced applications of micro and nano clay II: synthetic polymer composites. *In: Materials Research Foundations*. Millersville, PA: Material Research Forum LLC; 2022. 290 p. <https://doi.org/10.21741/9781644902035>
14. Bel'chinskaya L. I., Khodosova N. A., Novikova L. A., Strel'nikova O. Y., Roessner F., Petukhova G. A., Zhabin A. V. Regulation of sorption processes in natural nanoporous aluminosilicates. 2. Determination of the ratio between active sites *Protection of Metals and Physical Chemistry of Surfaces*. 2016;52(4): 599–606. <https://doi.org/10.1134/s2070205116040055>
15. Khodosova N. A., Tomina E. V., Belchinskaya L. I., Zhabin A. V., Kurkin N. A., Volkov, A. S. Physical and chemical characteristics of the nanocomposite nontronite/ $\text{CoFe}_2\text{O}_4$  sorbent. *Sorbtsionnye i khromatograficheskie protsessy*. 2021;21(4): 520–528. (In Russ., abstract in Eng.). <https://doi.org/10.17308/sorpchrom.2021.21/3636>
16. JCPDC PCPDFWIN: A Windows retrieval/display program for accessing the ICDD PDF – 2 Data Base, International Centre for Diffraction Data, 1997.
17. Brandon D., Kaplan W.D. *Microstructural characterization of materials*. John Wiley & Sons Ltd; 1999. 409 p. <https://doi.org/10.1002/9780470727133>
18. The list of substances, products, production processes, domestic and natural factors that are carcinogenic to humans. GN 1.1.029-98. Moscow: Goskomsanepidnadzor Russia; 1995. 17 p.
19. Stefan W: *The Great Reference Book of Lapis Minerals. All minerals from A to Z and their properties. 5th edition completely revised and enlarged*. Weise, Munich 2008, ISBN 978-3-921656-70-9.
20. Nurizyanov R. M. *Geology minerals and rocks*. Almet'yevsk: Almet'yevsk State Oil Institute Publ., 2012. 84 p. (In Russ.)
21. Bergaya F., Lagaly G. *Handbook of Clay Science. Developments in Clay Science 5*. Amsterdam: Elsevier; 2013. 787 p. Available at: <https://www.sciencedirect.com/bookseries/developments-in-clay-science/vol/5/suppl/C>
22. Gorshkov V. S., Savelyev V. G., Fedorov N. F. *Physical chemistry of silicates and other refractory compounds*. Moscow: Vysshaya shkola Publ.; 1988. 400 p.
23. Krupskaya V. V., Zakusin S. V., Tyupina E. A., Dorzhieva O. V., Chernov M. S., Bychkova Ya. V. Transformation of structure and adsorption properties of montmorillonite under thermochemical treatment. *Geochemistry International*. 2019;57(3): 314–330. <https://doi.org/10.1134/s0016702919030066>

### Information about the authors

*Elena V. Tomina*, Dr. Sci. (Chem.), Head of the Department of Chemistry, Voronezh State University of Forestry and Technologies named after G. F. Morozov (Voronezh, Russian Federation).

[tomina-e-v@yandex.ru](mailto:tomina-e-v@yandex.ru)

<https://orcid.org/0000-0002-5222-0756>

*Nataliya A. Khodosova*, Cand. Sci. (Chem.), Associate Professor at the Department of Chemistry, Voronezh State University of Forestry and Technologies named after G. F. Morozov (Voronezh, Russian Federation).

[nhodosova@mail.ru](mailto:nhodosova@mail.ru)

<https://orcid.org/0000-0002-2809-717X>

*Alexander A. Sinelnikov*, Cand. Sci. (Phys.–Math.), Head of Laboratory, Department of Materials Science and Industry of Nanosystems, Voronezh State University (Voronezh, Russian Federation).

[rnileme@mail.ru](mailto:rnileme@mail.ru)

<https://orcid.org/0000-0002-0549-4615>

*Aleksandr V. Zhabin*, Cand. Sci. (Geology-Mineralogical), Associate Professor at the Department of General Geology and Geodynamics, Voronezh State University (Voronezh, Russian Federation).

[zhabin01@gmail.com](mailto:zhabin01@gmail.com)

<https://orcid.org/0000-0002-3844-6302>

*Nikolay A. Kurkin*, PhD student, Department of Materials Science and Industry of Nanosystems, Voronezh State University (Voronezh, Russian Federation).

[kurkin.nik@yandex.ru](mailto:kurkin.nik@yandex.ru)

<https://orcid.org/0000-0002-0468-8207>

*Lyudmila A. Novikova*, Cand. Sci. (Chem.), Associate Professor at the Department of Chemistry, Voronezh State University of Forestry and Technologies named after G. F. Morozov (Voronezh, Russian Federation).

[yonk@mail.ru](mailto:yonk@mail.ru)

<https://orcid.org/0000-0002-1635-7739>

Received 04.03.2022; approved after reviewing 15.03.2022; accepted for publication 15.05.2022; published online 25.09.2022.

Translated by Valentina Mittova

Edited and proofread by Simon Cox